Interpolation within ray tubes - state of the art

Petr Bulant
Department of Geophysics, Faculty of Mathematics and Physics, Charles University, Ke Karlovu 3, 121 16 Praha 2, Czech Republic,
http://sw3d.cz/staff/bulant.htm

Summary

Ray tracing followed by calculation of travel times and other quantities at specified points by means of interpolation within ray tubes is a method which was developed in the SW3D consortium several years ago. The emphasis was put on calculation of all existing ray–theory arrivals, and not the first arrivals only. The method was successfully applied by the SW3D researchers in many applications. The method was also described in several papers published in previous reports of the consortium and also in reviewed journals.

As the method appears recently to be of higher interest of at least some consortium members, we present here this paper, which aims to present a short description of the method, to briefly mention its numerical realization and the computer codes developed for the method, to give an overview of the recent applicability of the computer codes, to shortly mention the plans for future extension of the method, and to present the list of examples of the application of the method.

Keywords

Controlled initial–value ray tracing, interpolation within ray tubes, multivalued travel times, ray–theory Green tensor.

1. Basic principles of the method

The method of calculation of a seismic ray (or a set of rays) from given source under given initial conditions is called *initial–value ray tracing* (Červený, Klimeš & Pšenčík, 1988). Once a ray is calculated, it may be assigned *ray history* integer function, which is equal for the rays which pass the same model blocks, interact with the same interfaces, display the same behaviour at caustics, and terminate in the same area for the same reason.

In models with interfaces, not all rays pass through an equal sequence of blocks, interfaces and caustics. The continuity and smoothness of the travel time, its derivatives, spatial coordinates of rays, and many other quantities is violated between such rays. On the other hand, methods such as interpolation, paraxial ray approximation or perturbation expansion require smoothness and continuity of the above mentioned quantities. This smoothness is guaranteed within the rays of constant ray history. That is why the ray history is introduced, and why the regions of the same ray history are determined in the domain of ray take–off parameters.

In the *controlled initial–value ray tracing* (Bulant, 1999), the chosen domain of ray take–off parameters is covered by rays in order to identify regions of the same ray history. The boundaries between the regions with different values of the ray history

In: Seismic Waves in Complex 3-D Structures, Report 22 (Department of Geophysics, Charles University, Prague, 2012), pp. 169-182

are demarcated by pairs of *boundary rays*, which are two very close rays with different history. The emphasis is put on proper identification of the boundaries, and on keeping the demarcation belts formed by the pairs of boundary rays as narrow as possible. The regions of the same ray history are then sampled by *homogeneous triangles*, by which we understand triangles in the ray parameter domain whose vertices are given by ray parameters of rays with equal ray history. The homogeneous triangles should not be too different from equilateral. See Figures 1 to 3 for an illustration of identification of boundaries between ray histories and sampling the regions of the same ray history by homogeneous triangles.

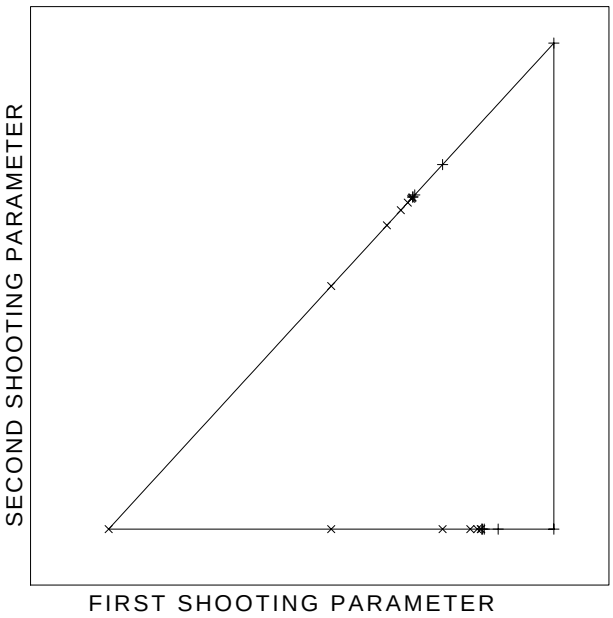

Figure 1: A triangle in the ray parameter domain is formed by three *basic rays* traced for the basic estimation of the distribution of the ray histories. The rays are symbol–coded according to their history. As the vertices of the triangle display different ray history, searching for *boundary rays* (two close rays with different history) on the sides of the triangle by halving intervals is applied. Note that the distance between the two rays in each pair of boundary rays is very small.

Controlled initial–value ray tracing has many applications: it is the basis of boundary–value (two–point) ray tracing, it serves as the preprocessor for interpolation within ray tubes, it is applied in wavefront tracing, and it is of principal importance in the asymptotic summation of Gaussian beams or in the asymptotic summation of Gaussian packets.

Each triplet of rays corresponding to the vertices of a homogeneous triangle generate a *ray tube* through the model volume. Each traced ray is recorded as a set of points of two types. First, there are the points on the ray stored with a given travel–time step; we shall refer to them as *time points*. Second, there are the points of interaction of the ray with interfaces and other surfaces (reflection, transmission or termination); we shall refer to them as *interaction points*. A ray tube is thus represented as a set of the above points on the three rays, which form the ray tube, see Figure 4.

Interpolation within ray tubes (Bulant & Klimeš, 1999) may be then used to compute all the quantities already calculated along the rays to any point located within the ray tube. For interpolation, the ray tube is decomposed into *ray cells*. *Regular ray cells*

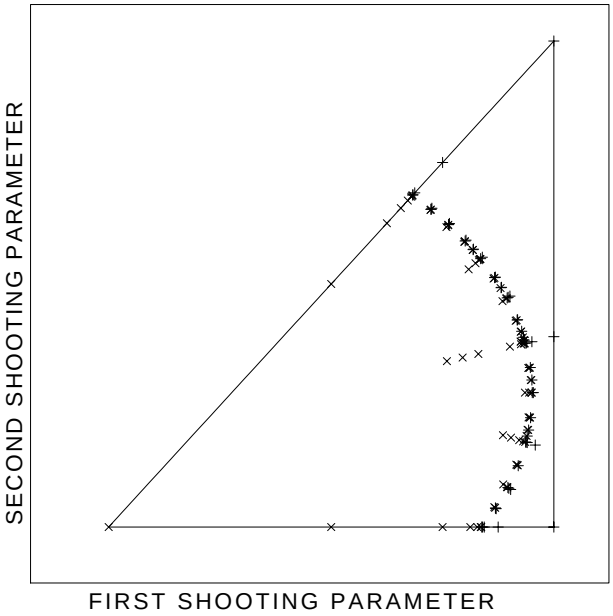

Figure 2: The boundary between the two ray histories is demarcated by pairs of boundary rays. All the boundary and basic rays of the same ray history create a homogeneous polygon. Here are two homogeneous polygons, which will be divided into homogeneous triangles in the next step.

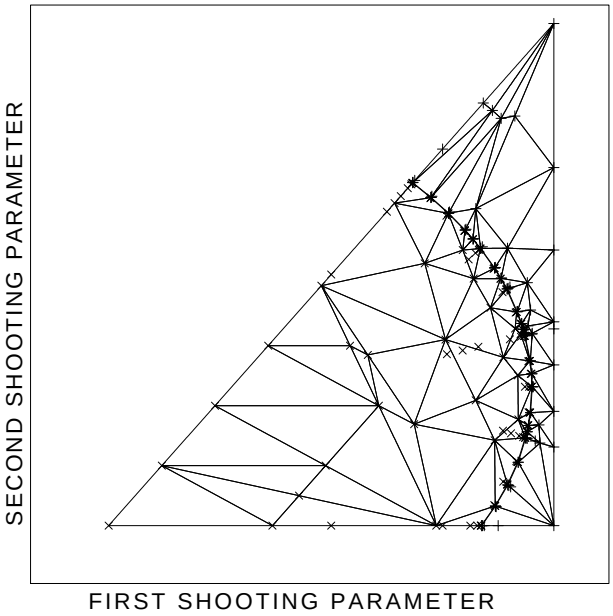

Figure 3: Both homogeneous polygons are covered by homogeneous triangles. Each homogeneous triangle is formed by three rays of equal ray history. Several new rays were traced in order to create homogeneous triangles "not too different" from equilateral.

are defined by six points on the rays. Both the bottom and the top of the regular ray cell are formed by triangles defined by three points on the rays. These are usually the time points of the same travel–time level. *Degenerate ray cells* are formed by five or four points. They occur at a point source, where the bottom of a ray cell is formed by a single point, in front of and beyond interfaces, where one or two points of the top of a ray cell coincide with the corresponding point(s) of the bottom, and in front of the end surface where the ray tube terminates, see again Figure 4.

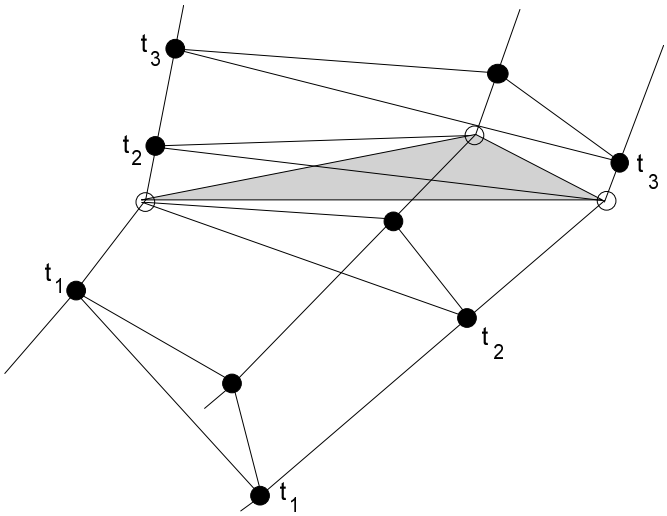

Figure 4: Decomposition of a ray tube into ray cells. Three rays, forming a ray tube, cross an interface. Bullets represent the points at three travel–time levels t_1, t_2 and t_3 ("time points"). Circles are the points of intersection of the rays with the interface ("interaction points"). Starting from the bottom of the figure, we can see one regular ray cell formed by six points, then two degenerate cells formed by five and four points, and again a regular ray cell. The bottom of the first ray cell and the top of the fourth cell are formed by triangles which approximate wavefronts at travel-time levels t_1 and t_3. The shaded triangle, which is the top of the second cell and the bottom of the third cell, approximates the interface.

Once a ray tube is decomposed into the ray cells, we may proceed to interpolation within individual ray cells. We identify the target points located within the ray cell, and then we can interpolate all the required quantities from the values at the vertices of the ray cell to the target points. The interpolation algorithm by Bulant & Klimeš (1999) incorporates both the decision whether a receiver lies in the ray cell and the interpolation to the receiver. It is applicable to all ray cells formed by six, five or four points. All the quantities computed along rays may be interpolated, using the values of the quantities only at the vertices of the corresponding ray cell.

We mentioned here briefly only the basic principles of the method. For the detailed description of the method, refer to papers by Bulant (1999) and Bulant & Klimeš (1999). The principles of the method are also very precisely explained in the Chapter 4 of a review paper by Červený, Klimeš & Pšenčík (2007).

2. Numerical realization and the computer codes developed for the method

Within the software packages FORMS, MODEL and CRT developed by the SW3D consortium, the interpolation within ray tubes is realized in two steps. In the first step, the controlled initial–value ray tracing is performed by running the computer code `crt.for`. During this step, a set of rays which cover the model volume by ray tubes is calculated, and the calculated rays are stored in the output files of the `crt.for` program. In the second step, the code `mtt.for` reads the calculated rays and performs the interpolation within the ray tubes.

2.1. Models for ray tracing

Software package MODEL is used for description of models for ray tracing. General 3-D layered and block isotropic or anisotropic structures, containing isolated bodies, pinchouts, etc., may be modelled. Attenuation and non-planar topography can be considered.

Inside the layers and blocks, the elastic parameters may vary smoothly in all three dimensions. The elastic parameters may be discontinuous only along structural interfaces.

The structural interfaces are composed of one or several smooth surfaces or of parts thereof. The surfaces forming the interfaces are defined implicitly, as the zero isosurfaces of given functions.

2.2. Calculation of rays - program `crt.for`

Program `crt.for` may be used for ray tracing of P and S waves in general 3-D layered and block isotropic structures. It may be used also for P-wave ray tracing in anisotropic structures without interfaces, and for the calculation of common S-wave rays in anisotropic structures without interfaces (Klimeš, 2006). The quantities calculated along rays may be stored in the output files with given time step, and the quantities at structural interfaces and at the end surface are stored as well. Also the file with the indices of the rays corresponding to the vertices of homogeneous triangles (i.e. ray tubes) is stored. The quantities stored in the points along rays include coordinates, ray history, travel time and its derivatives, ray propagator matrix, and amplitudes of the Green function.

Of the input parameters of `crt.for`, let us mention several parameters most important for the controlled initial–value ray tracing: The width of the demarcation belts between the ray histories (i.e. the distance of boundary rays in the ray–parameter domain, see Figure 2) is controlled by parameter AERR; parameter PRM0(3) influences the information included in calculation of ray histories; parameter PRM0(4) influences the width of the ray tubes.

Note that in the case of common S-wave rays in smooth anisotropic structures, the rays calculated by `crt.for` may be used for calculation of Green functions of both S-wave rays using the coupling ray theory by program `green.for`. The coupling ray theory is unfortunately not yet incorporated within the interpolation program `mtt.for`, and, in the case of S-wave rays in anisotropic structures, the current version of `mtt.for` can thus be used only for interpolation of quantities calculated along common S-wave rays, namely for interpolation of average travel time of the two S waves.

2.3. Interpolation within ray tubes - program `mtt.for`

Program `mtt.for` reads the file with homogeneous triangles and the files with quantities calculated by `crt.for` and stored along the rays. Each ray tube formed by three rays - the vertices of a selected homogeneous triangle - is divided by consecutive wavefronts or structural interfaces into ray cells whose vertices are formed by three points on the three rays in a given time level (or interface), and by the three points in the next time level or interface, see Figure 4. The quantities stored along the rays are then interpolated within each ray cell according to Bulant & Klimeš (1999) using bicubic interpolation for the travel time and bilinear interpolation for other quantities.

The quantities may be interpolated to the gridpoints of arbitrary regular rectangular 3-D grid of points, or to the individual points specified in an input file. The following quantities may be interpolated:

- number of arrivals at each point
- real and imaginary travel times of all determined arrivals
- ray history
- slowness vector
- second derivatives of travel time with respect to the coordinates of the point
- components of the 4×4 ray propagator matrix in ray–centred coordinates
- sum of squares of Gaussian beam widths (for Gaussian beam migrations)
- real or imaginary part of the vectorial amplitude of the Green function, norm of the vectorial amplitude of the Green function, and amplitude modified for use in the Kirchoff integral
- coordinates of the initial point of the ray corresponding to the arrival (suitable mostly for linear or planar sources)
- derivatives of travel time with respect to the coordinates of the source (i.e. the vector opposite to the slowness vector in the source)

During the interpolation to the regular rectangular grids, the interpolated quantities are stored in individual output files. During the interpolation to the points of given coordinates just one output file is generated with the interpolated quantities written in individual columns of the file. The written quantities may be sorted according to a selected quantity in an ascending or descending order (usually sorting according to the travel time is used).

Note that programs `crt.for` and `mtt.for` may also be used for 2-D calculation of rays followed by interpolation between the rays (i.e. within 2-D "ray tubes" formed by two neighbouring rays), the quantities are then interpolated at the points projected onto the 2-D system of rays along a given projection vector. Similar computation may be realized using the program `crt2d3d.for` to transform 2-D system of rays into 3-D system of rays by shifting the 2-D set of rays along a given translation vector, followed by 3-D interpolation within the newly created 3-D system of rays.

2.4 Further processing of the interpolated quantities

Interpolation within ray tubes is most frequently performed to the gridpoints of regular rectangular grids. Several programs were coded for further calculations with the gridded data obtained by interpolation. Let us briefly mention at least the most frequently used ones:

- program `grdborn.for` to calculate the Born approximation of the wavefield at specified receivers
- program `mgrd.for` is designed to convert a multivalued grid into several singlevalued grids;
- program `mttgrd.for` is designed to convert a multivalued grid into several singlevalued grids sorted according to the ray history;
- program `grdcal.for` to perform vectorial calculations with singlevalued gridded data enables to perform all the basic operations like addition, subtraction, multiplication, division, exponentiation, logarithms, goniometric functions, and many other operations;
- program `grdnorm.for` to calculate the spatial density of the Lebesgue norm of gridded data, mostly used for calculation of maximum or average value of the gridded data;
- program `grdps.for` to display gridded data in PostScript;
- program `grdmigr.for` to perform common-source Kirchhoff migration using gridded travel times and amplitudes.

For the other programs refer to package FORMS (http://sw3d.cz/software/sw3dcd15/forms/forms.htm). Note that program `mtt.for` stores the output quantities in the form of multivalued grids, which may be recently directly processed only by program `grdborn.for`. For the other programs, the multivalued grids must be converted into singlevalued grids using programs `mgrd.for` or `mttgrd.for`.

3. Applicability of the method

Let us once again summarize that the computer codes are currently applicable to isotropic P and S waves in general 3-D block velocity models, to P waves in smooth 3-D anisotropic velocity models, and to common S waves in smooth anisotropic structures. The quantities may be interpolated either to gridpoints of regular rectangular grid, or to the individually specified points. In 2-D, the codes may be used either by means of projection of the target points onto the 2-D system of rays, or by the extension of the 2-D system of rays into the 3-D system of rays.

4. Future plans

Application of the coupling ray theory, which is recently used in program `green.for` for calculation of the Green function, is planned within the program `mtt.for`, which would make interpolation within ray tubes possible also for S waves in smooth weakly anisotropic structures. Incorporation of the single–frequency approximation of the coupling ray theory (Klimeš & Bulant, 2012) into the program `mtt.for` should be straightforward. Tracing of the anisotropic P-wave and anisotropic common S-wave rays in models with structural interfaces is also planned.

5. Numerical examples

In this section we give the list of the numerical examples in which interpolation within ray tubes is used, and then we give more detailed description of two of the examples.

5.1. List of the numerical examples

Package DATA (http://sw3d.cz/software/sw3dcd15/data/data.htm) consists of the numerical examples of the calculations performed by the SW3D researchers in the past years. The package is sorted according to the models used for the calculations. In the numerical examples, individual programs are run according to the so-called *history files*. The history files are designed to contain both the data for the calculation and the information how to execute the programs, brief comments about the calculations are usually also included. Let us now give a list of all the history files of package DATA in which program `mtt.for` is executed. In the list we first give the name of the model and then the name of the history file:

`len/leni-mtt.h`
: 3-D model, 2-D target grid,
calculation of travel times,
pictures of travel times sorted according to their value

`hes/hes-mtt.h`
: 2-D model, 2-D target grid,
calculation of travel times,
pictures of rays together with the numbers of arrivals, pictures of travel times sorted according to their value or according to the ray history

`mar/mar-crt.h`
: 2-D model, 2-D target grid,
calculation of numbers of arrivals and the widths of Gaussian beams

`mar/mar-mcrt.h`
: 2-D model, 2-D target grid,
calculation of numbers of arrivals, travel times, and amplitudes for Kirchhoff migration (sorting according to amplitudes)
optional pictures of rays together with the numbers of arrivals, and of travel times sorted according to their value

`mar/mgb-opt1.h`
: 2-D model, 2-D target grid,
calculation of travel times as an input for calculation of optimum initial parameters of Gaussian beams

`mar/mgp-mig1.h`
: 2-D model, 2-D target grid,
calculation of travel times and amplitudes for Gaussian packet migration

`p1i/p1-mtt.h`
: 2-D model, 2-D target grid,
calculation of slowness vectors, travel times and ray amplitudes,
pictures of rays together with velocity, model block indices, and numbers of arrivals

`born/m2d-mtt.h`
: 2-D model, 2-D target grid,
calculation of slowness vectors, travel times and amplitudes for Born approximation

`vgr/vgr-q2.h`
: 1-D constant velocity gradient model, 2-D target grid,
calculation of geometrical spreading from gridded slowness vectors

`wb/wb2-loc.h`
: 3-D model, 3-D target grid,
calculation of travel times for kinematic hypocentre determination

`98/98-mtt.h`
: 3-D model, 2-D target grid,
calculation of travel times,
pictures of travel times sorted according to their value or according to the ray history

5.2. History file `mar-mcrt.h`

History file `mar-mcrt.h` controls the calculation of travel times and amplitudes in the smoothed version of 2-D Marmousi model. Figure 5 shows the colour–coded slowness in the model together with the 2-D system of rays traced during the controlled initial–value ray tracing. The calculation of rays is terminated at maximum travel time of 2.3 s, which is visible at the top left and top right corners of the figure. Two larger caustics and a third small caustic are visible on the ray field.

Figure 6 shows the colour–coded numbers of arrivals. There are mostly single arrivals identified at the gridpoints (marked by green). No arrivals (marked by yellow) were calculated in the corners of the model, either due to the termination of calculation of rays at the 2.3 s isochrone visible at the top corners of the model, or due to the termination of rays at the boundaries of the model in the lower corners of the model. No interpolation was performed in the first ray cell of each ray tube, creating the yellow half–circle around the source. Red colour shows the gridpoints with three arrivals caused by the caustics. There are also several gridpoints with two arrivals (marked by blue) in the area of the top left caustic behind the 2.3 s isochrone.

Figure 7 shows colour–coded travel times calculated in the Marmousi model. The top figure shows the first arrival to the gridpoints, and the middle and bottom figures show the second and third arrival between the caustics.

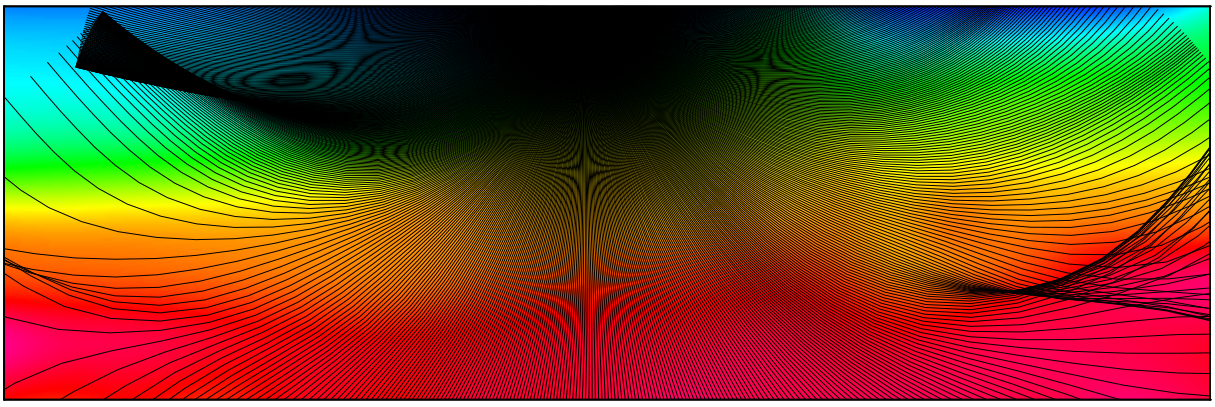

Figure 5: P-wave slowness in the smooth 2-D model Marmousi, together with the 2-D system of rays traced during the controlled initial–value ray tracing from the source. The P-wave slowness ranges from 0.000653 s/km shown in blue to 0.000226 s/km shown in red. The whole colour circle corresponds to the interval of 0.000581 s/km.

Figure 6: Numbers of arrivals interpolated in model Marmousi. The numbers of arrivals range from 0 displayed in yellow through 1 in green, 2 in blue to 3 shown in red.

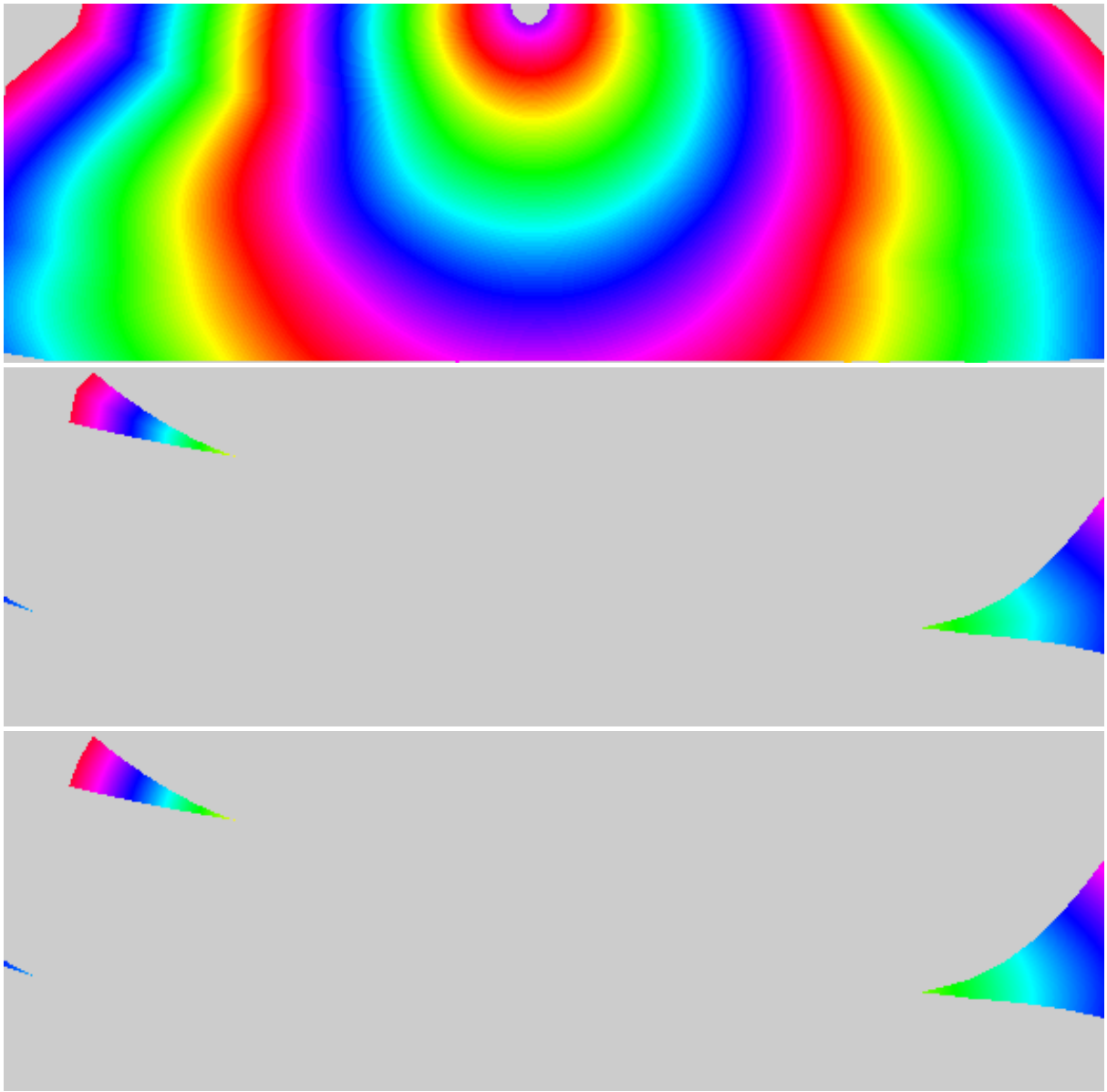

Figure 7: Travel times calculated during the interpolation within the ray tubes in model Marmousi. The whole colour circle corresponds to the interval of 1 s. The travel times are sorted according to their value, i.e. the first picture shows the fastest arrival and the last picture shows the latest arrival to the gridpoints. In other words, the first picture shows the first arrival, and the other two pictures show the second and third arrivals between the caustics.

5.3. History file `p1-mtt.h`

Model P1 created by Bulant & Martakis (2011) is a smooth 2-D model used by Šachl (2011, 2012a, 2012b) as the background model for Born approximation. As an input for the Born approximation, Green functions need to be calculated both from the source and from the receiver to the gridpoints of the target grid covering the area of the model where the reflection surfaces are located. The calculation is performed in the smooth version P1 of the model, and is run according to the history file `p1-mtt.h`. History file `p1-mtt.h` generates also several figures with calculated rays, numbers of arrivals and calculated travel times.

Figure 8 shows colour–coded velocity of the P-wave in the smooth 2-D model P1 calculated by history file `p1-grid.h`, together with the 2-D system of rays traced during the controlled initial–value ray tracing from the source, the source is marked by asterix. We can see the development of the caustics caused by lateral heterogeneities in the model. Figure 9 shows colour–coded numbers of arrivals calculated by interpolation within 2-D ray tubes composed by the displayed system of rays traced from the source. Figure 10 shows travel times calculated by the interpolation, sorted according to their value. Figure 11 shows the same travel times, but sorted according to the ray history.

Figures 12 to 15 are analogous to Figures 8 to 11, but for the rays calculated from the receiver.

Note that there should always be at least one arrival in the unbounded smooth medium. Only the boundaries of the model may create shadows with no arrival in such a medium. This is the case of the described model, where negative velocity gradient near the surface of the model creates large area with no arrival, marked by yellow colour in Figures 9 and 13. These areas with no arrival are thus caused by the shadow of the model boundary, and not by a failure of the described method.

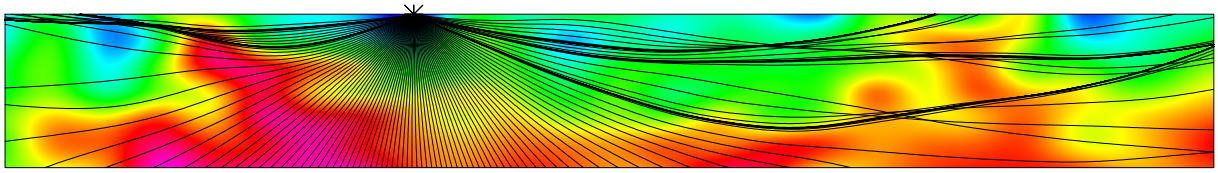

Figure 8: P-wave velocity in the smooth one-block model P1, together with the 2-D system of rays traced during the controlled initial–value ray tracing from the source. The source is marked by asterix. The P-wave velocity ranges from 4.64 km/s shown in blue to 5.93 km/s shown in magenta. The whole colour circle corresponds to the interval of 1.50 $\mathrm{km\,s^{-1}}$.

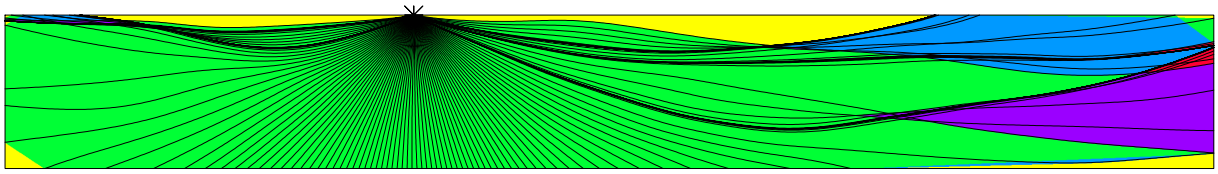

Figure 9: Numbers of arrivals interpolated in the smooth one-block model P1, together with the 2-D system of rays from the source. The numbers of arrivals range from 0 displayed in yellow through 1 in green, 2 in blue, 3 in violet to 4 shown in red. Zero arrival numbers at the upper part of the model are caused by the negative velocity gradient at the top of the model.

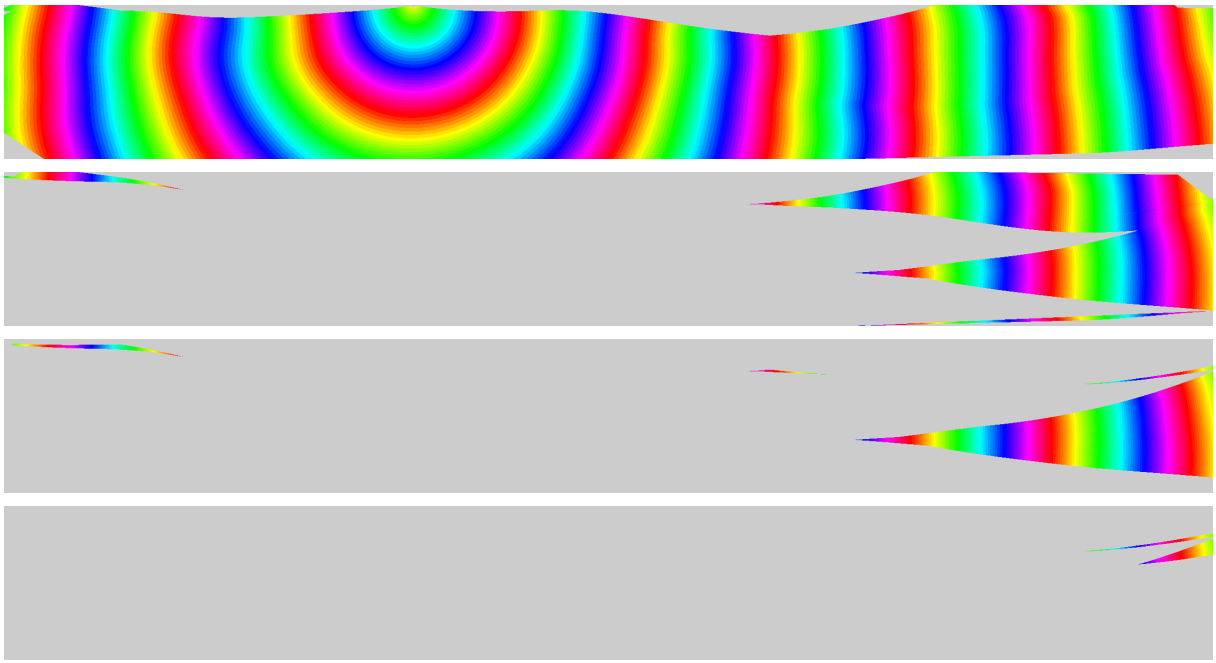

Figure 10: Travel times calculated during the interpolation within the ray tubes formed by the rays traced from the source. The whole colour circle corresponds to the interval of 1 s. The travel times are sorted according to their value, i.e. the first picture shows the fastest arrival and the last picture shows the latest arrival to the gridpoints.

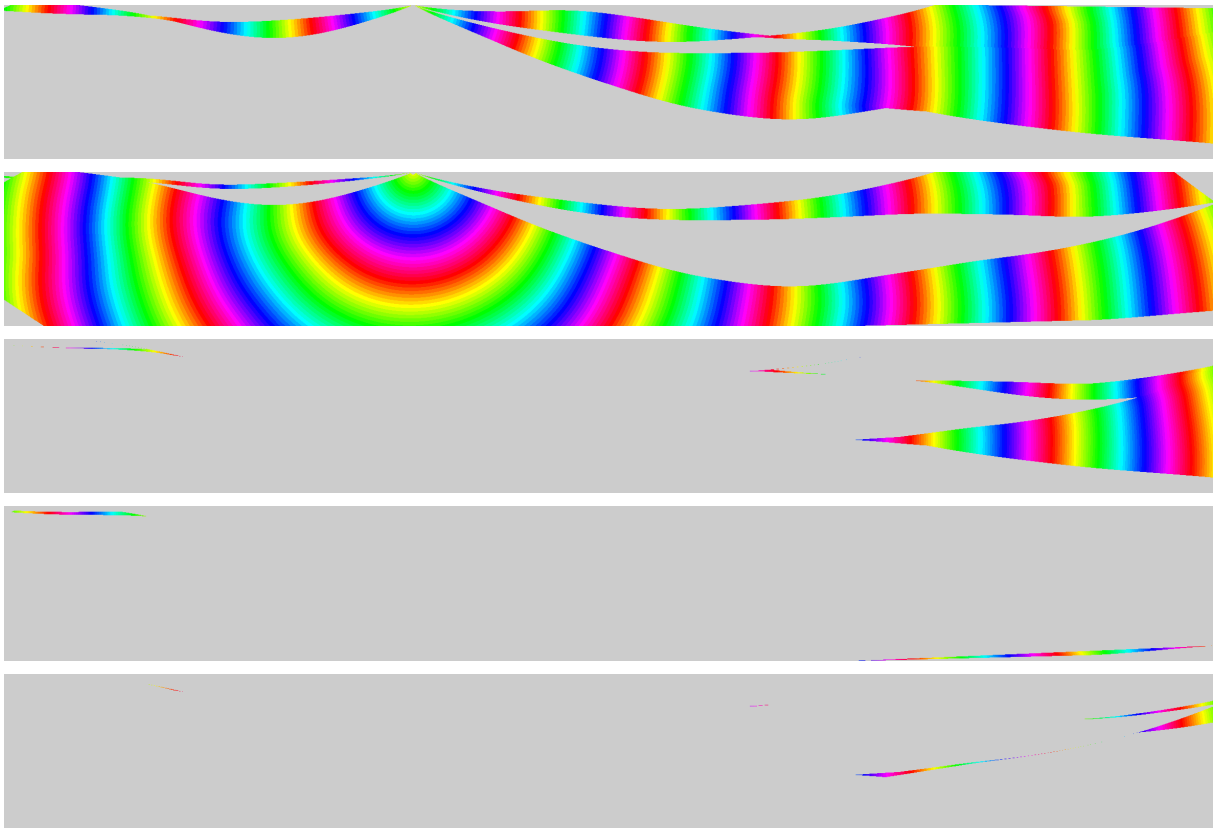

Figure 11: Travel times calculated during the interpolation from the source. The travel times are sorted according to the ray history.

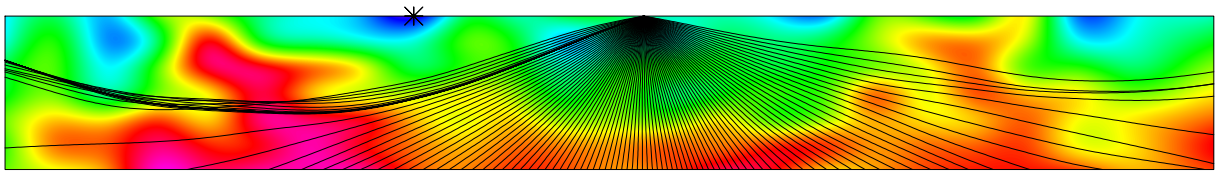

Figure 12: P-wave velocity in the smooth one-block model P1, together with the 2-D system of rays traced from the receiver. The source is marked by asterix. The P-wave velocity ranges from 4.64 km/s shown in blue to 5.93 km/s shown in magenta. The whole colour circle corresponds to the interval of 1.50 $\mathrm{km\,s^{-1}}$.

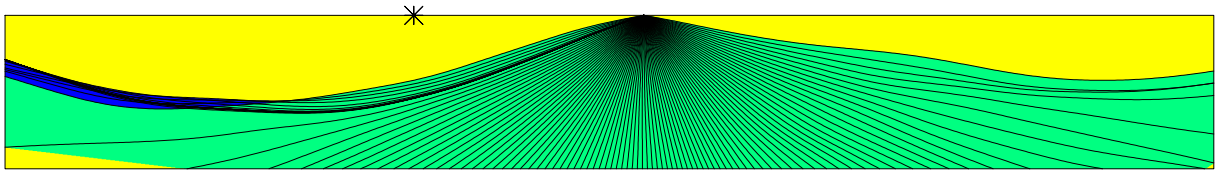

Figure 13: Numbers of arrivals interpolated in the smooth one-block model P1, together with the 2-D system of rays from the receiver. The numbers of arrivals range from 0 displayed in yellow through 1 in green to 2 in blue. Zero arrivals at the upper part of the model are caused by the negative velocity gradient at the top of the model.

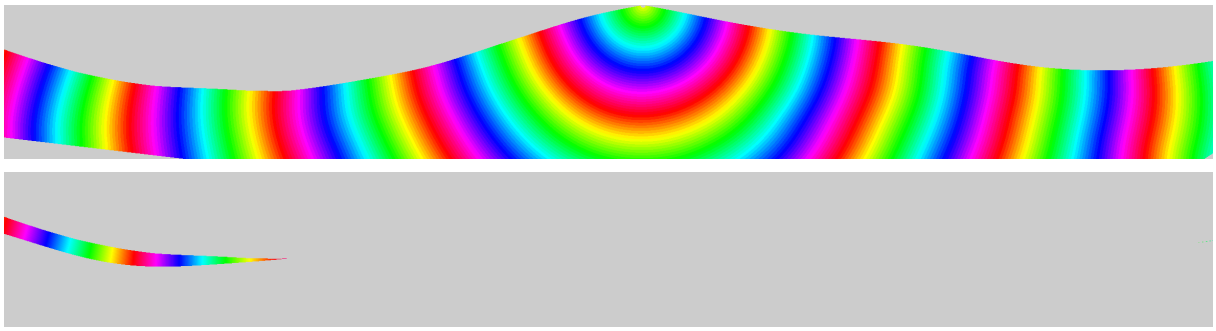

Figure 14: Travel times calculated during the interpolation within the ray tubes formed by the rays traced from the receiver. The whole colour circle corresponds to the interval of 1 s. The travel times are sorted according to their value.

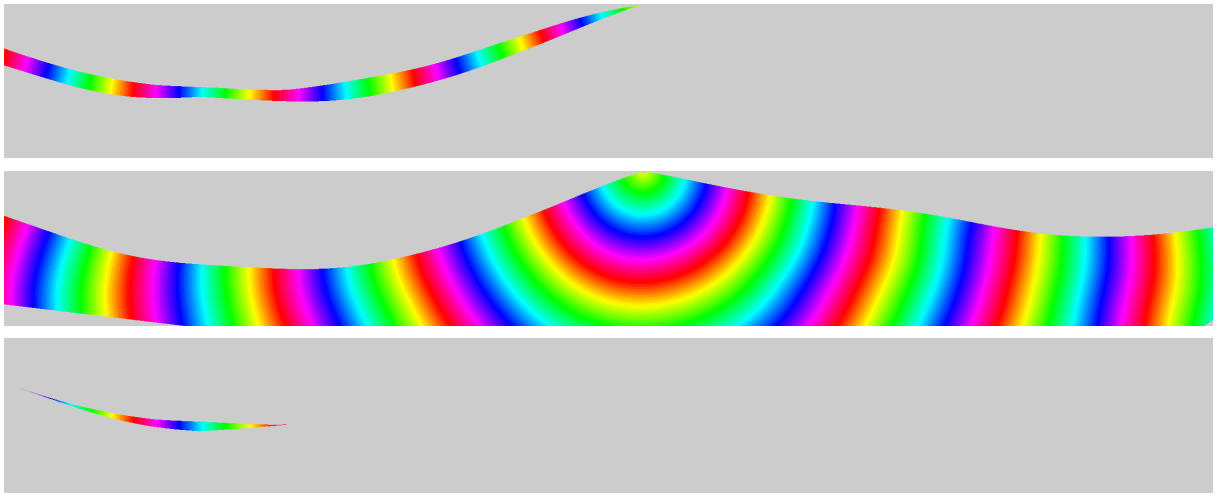

Figure 15: Travel times calculated during the interpolation from the receiver. The travel times are sorted according to the ray history.

Acknowledgements

Velocity data for model P1I were provided by Stream Oil & Gas Ltd. The research has been supported by the Grant Agency of the Czech Republic under Contract P210/10/0736, by the Ministry of Education of the Czech Republic within research project MSM0021620860, and by the members of the consortium "Seismic Waves in Complex 3-D Structures" (see "http://sw3d.cz").

References

Bulant, P. (1999): Two–point ray–tracing and controlled initial–value ray–tracing in 3-D heterogeneous block structures. *J. seism. Explor.*, **8**, 57–75.

Bulant, P. & Klimeš, L. (1999): Interpolation of ray theory traveltimes within ray cells. *Geophys. J. int.*, **139**, 273–282.

Bulant, P. & Martakis, N. (2011): Constructing model P1I for reflection studies. In: *Seismic Waves in Complex 3-D Structures, Report 21*, pp. 17–25, Dep. Geophys., Charles Univ., Prague, online at "http://sw3d.cz".

Červený, V., Klimeš, L. & Pšenčík, I. (1988): Complete seismic–ray tracing in three–dimensional structures. In: Doornbos, D.J. (ed.): *Seismological Algorithms*, pp. 89–168, Academic Press, New York.

Červený, V., Klimeš, L. & Pšenčík, I. (2007): Seismic ray method: Recent developments. *Advances in Geophysics*, **48**, 1–126.

Klimeš, L. (2006): Common–ray tracing and dynamic ray tracing for S waves in a smooth elastic anisotropic medium. *Stud. geophys. geod.*, **50**, 449–461.

Klimeš, L. & Bulant, P. (2012): Single–frequency approximation of the coupling ray theory. In: *Seismic Waves in Complex 3-D Structures, Report 22*, pp. 143–167, Dep. Geophys., Charles Univ., Prague, online at "http://sw3d.cz".

Šachl, L. (2011): Born approximation in heterogenous model P1. In: *Seismic Waves in Complex 3-D Structures, Report 21*, pp. 99–114, Dep. Geophys., Charles Univ., Prague, online at "http://sw3d.cz".

Šachl, L. (2012a): Effect of caustics to the ray–based Born approximation. In: *Seismic Waves in Complex 3-D Structures, Report 22*, pp. 55–82, Dep. Geophys., Charles Univ., Prague, online at "http://sw3d.cz".

Šachl, L. (2012b): Born and ray–theory seismograms in 2D heterogenous isotropic models. In: *Seismic Waves in Complex 3-D Structures, Report 22*, pp. 83–112, Dep. Geophys., Charles Univ., Prague, online at "http://sw3d.cz".